

BRAIN COMMUNICATIONS

REPORT

Biallelic *NDUFA13* variants lead to a neurodevelopmental phenotype with gradual neurological impairment

 **Rauan Kaiyrzhanov,^{1,2} Kyle Thompson,³  Stephanie Efthymiou,¹  Askhat Mukushev,⁴ Akbota Zharylkassyn,⁵ Chitra Prasad,⁶ Ehsan Ghayoor Karimiani,^{1,7} Javeria Raza Alvi,⁸ Dmitriy Niyazov,⁹ Ahmad Alahmad,¹⁰ Meisam Babaei,¹¹ Homa Tajsharghi,¹² Buthaina Albash,¹³ Ahmad Alaqeel,¹³ Majida Charif,^{14,15,16} Narges Hashemi,¹⁷ Morteza Heidari,¹⁸ Seyed Mehdi Kalantar,¹⁹ Guy Lenaers,^{20,21} Mohammad Yahya Vahidi Mehrjardi,²² Varunvenkat M. Srinivasan,²³  Vykuntaraju K. Gowda,²³ Seyed Hamidreza Mirabutalebi,¹⁹ Deanna Alexis Carere,²⁴ Mojtaba Movahedinia,²⁵ David Murphy,²⁶ Robert McFarland,^{3,27} Mohamed S. Abdel-Hamid,²⁸ Rasha M. Elhossini,²⁹ Shahryar Alavi,¹ Melanie Napier,²⁴ Amaya Belanger-Quintana,³⁰ Asuri N. Prasad,³¹ Jessica Jakobczyk,⁶ Agathe Roubertie,³² Tony Rupar,^{33,34} Tipu Sultan,⁸ Mehran Beiraghi Toosi,^{17,35} Leonid Sazanov,³⁶  Mariasavina Severino,³⁷  Henry Houlden,¹ Robert W. Taylor^{3,27} and  Reza Maroofian¹**

Biallelic variants in NADH (nicotinamide adenine dinucleotide (NAD) + hydrogen (H))-ubiquinone oxidoreductase 1 alpha subcomplex 13 have been linked to mitochondrial complex I deficiency, nuclear type 28, based on three affected individuals from two families. With only two families reported, the clinical and molecular spectrum of NADH-ubiquinone oxidoreductase 1 alpha subcomplex 13-related diseases remains unclear. We report 10 additional affected individuals from nine independent families, identifying four missense variants (including recurrent c.170G > A) and three ultra-rare or novel predicted loss-of-function biallelic variants. Updated clinical–radiological data from previously reported families and a literature review compiling clinical features of all reported patients with isolated complex I deficiency caused by 43 genes encoding complex I subunits and assembly factors are also provided. Our cohort (mean age 7.8 ± 5.4 years; range 2.5–18) predominantly presented a moderate-to-severe neurodevelopmental syndrome with oculomotor abnormalities (84%), spasticity/hypertonia (83%), hypotonia (69%), cerebellar ataxia (66%), movement disorders (58%) and epilepsy (46%). Neuroimaging revealed bilateral symmetric T2 hyperintense substantia nigra lesions (91.6%) and optic nerve atrophy (66.6%). Protein modeling suggests missense variants destabilize a critical junction between the hydrophilic and membrane arms of complex I. Fibroblasts from two patients showed reduced complex I activity and compensatory complex IV activity increase. This study characterizes NADH-ubiquinone oxidoreductase 1 alpha subcomplex 13-related disease in 13 individuals, highlighting genotype–phenotype correlations.

- 1 Department of Neuromuscular Diseases, Queen Square Institute of Neurology, University College London, London WC1N 3BG, UK
- 2 Department of Neurology, South Kazakhstan Medical Academy, Shymkent 160019, Kazakhstan
- 3 Mitochondrial Research Group, Translational and Clinical Research Institute, Faculty of Medical Sciences, Newcastle University, Newcastle upon Tyne NE2 4HH, UK
- 4 Department of Neurology, Beth Israel Deaconess Medical Center, Harvard Medical School, Boston, MA 02215-5400, USA

Received July 02, 2024. Revised October 24, 2024. Accepted December 12, 2024. Advance access publication December 17, 2024

© The Author(s) 2024. Published by Oxford University Press on behalf of the Guarantors of Brain.

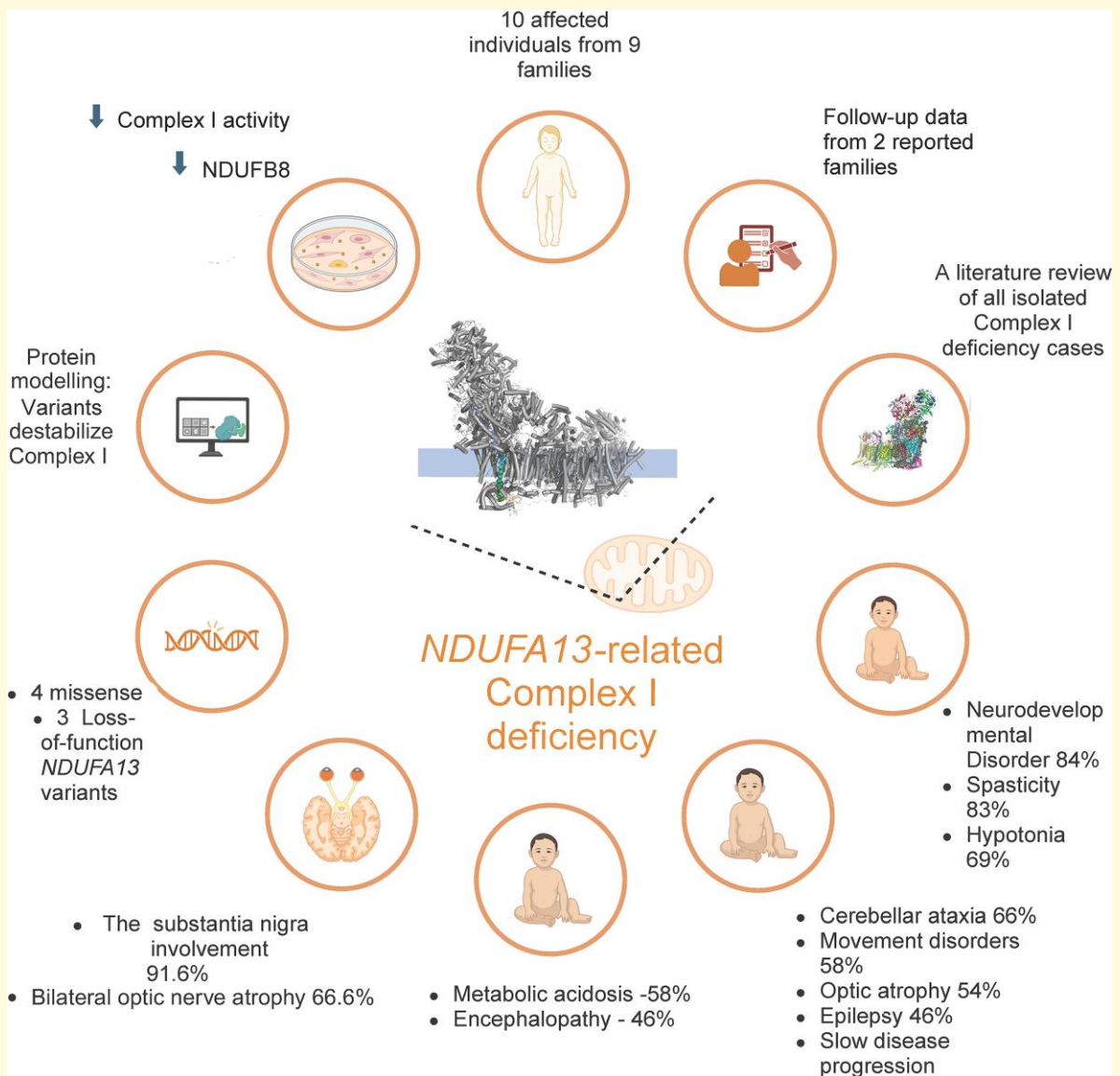
This is an Open Access article distributed under the terms of the Creative Commons Attribution License (<https://creativecommons.org/licenses/by/4.0/>), which permits unrestricted reuse, distribution, and reproduction in any medium, provided the original work is properly cited.

- 5 The Institute of Childhood Neurology, Almaty 050000, Kazakhstan
- 6 Division of Genetics and Metabolics, Department of Pediatrics, London Health Sciences, London, ON, Canada N6A 5W9
- 7 Molecular and Clinical Sciences Institute, St. George's University of London, London SW17 0RE, UK
- 8 Department of Pediatric Neurology, Children's Hospital and Institute of Child Health, Lahore 54000, Pakistan
- 9 Department of Pediatrics, Duke University School of Medicine, Durham, NC 27710, USA
- 10 Molecular Genetics Laboratory, Kuwait Medical Genetics Center, Ministry of Health, Sulaibikhat 80901, Kuwait
- 11 Department of Pediatrics, North Khorasan University of Medical Sciences, Bojnurd 9413813965, Iran
- 12 School of Health Sciences, Division of Biomedicine, University of Skovde, Skovde 541 28, Sweden
- 13 Kuwait Medical Genetics Centre, Al-Sabah Medical Area, Kuwait City 80901, Kuwait
- 14 Genetics Unit, Medical Sciences Research Laboratory, Faculty of Medicine and Pharmacy, University Mohammed Premier, Oujda 60000, Morocco
- 15 BRO Biobank, Faculty of Medicine and Pharmacy, University Mohammed Premier, Oujda 60000, Morocco
- 16 Genetic and Immuno-Cell Therapy Team, Mohammed First University, Oujda 60000, Morocco
- 17 Department of Pediatrics, School of Medicine, Mashhad University of Medical Sciences, Mashhad 91778 99191, Iran
- 18 Myelin Disorders Clinic, Department of Pediatric Neurology, Children's Medical Center, Pediatrics Center of Excellence, Tehran University of Medical Sciences, Tehran 14197 33151, Iran
- 19 Abortion Research Centre, Yazd Reproductive Sciences Institute, Shahid Sadoughi University of Medical Sciences, Yazd 8916188635, Iran
- 20 Angers University, MitoLab Team, MitoVasc Unit, CNRS UMR6015, INSERM U1083, SFR ICAT, Angers 49035, France
- 21 Department of Neurology, University Hospital of Angers, Angers 49035, France
- 22 Diabetes Research Center, Shahid Sadoughi University of Medical Sciences, Yazd 8916188635, Iran
- 23 Department of Pediatric Neurology, Indira Gandhi Institute of Child Health, Bangalore 560 029, India
- 24 GeneDx Inc., Gaithersburg, MD 20877, USA
- 25 Children Growth Disorder Research Center, Shahid Sadoughi University of Medical Sciences, Yazd 8916188635, Iran
- 26 Department of Clinical and Movement Neurosciences, UCL Queen Square Institute of Neurology, London WC1N 3BG, UK
- 27 NHS Highly Specialised Service for Rare Mitochondrial Disorders, Newcastle upon Tyne Hospitals NHS Foundation Trust, Newcastle upon Tyne NE1 4LP, UK
- 28 Medical Molecular Genetics Department, Human Genetics and Genome Research Institute, National Research Centre, Cairo 12622, Egypt
- 29 Clinical Genetics Department, Human Genetics and Genome Research Institute, National Research Centre, Cairo 12622, Egypt
- 30 Servicio de Pediatría, Enfermedades Metabólicas Hereditarias, Hospital Universitario Ramón y Cajal, Madrid 28034, Spain
- 31 Division of Pediatric Neurology, Department of Pediatrics, Western University, London, ON, Canada N6A 5W9
- 32 Department of Neuropaediatrics, Gui de Chauliac Hospital, Montpellier University Hospital, Institut des Neurosciences, INSERM U 1298, Montpellier 34091, France
- 33 Department of Pediatrics, University of Western Ontario, London, ON, Canada N6A5W9
- 34 Departments of Biochemistry, Pathology and Laboratory Medicine, University of Western Ontario, London, ON, Canada N6A5W9
- 35 Neuroscience Research Center, Mashhad University of Medical Sciences, Mashhad 91778 99191, Iran
- 36 Institute of Science and Technology Austria, Klosterneuburg A-3400, Austria
- 37 Neuroradiology Unit, IRCCS Istituto Giannina Gaslini, Genoa 16147, Italy

Correspondence to: Reza Maroofian
 Department of Neuromuscular Diseases
 UCL Queen Square Institute of Neurology
 London WC1N 3BG, UK
 E-mail: r.maroofian@ucl.ac.uk

Keywords: complex I deficiency; mitochondrial disorders; NDUFA13; neurodevelopmental disorder; Leigh syndrome

Graphical Abstract



Introduction

NADH (nicotinamide adenine dinucleotide (NAD) + hydrogen (H))-ubiquinone oxidoreductase 1 alpha sub-complex 13 (*NDUFA13*) (MIM*609435) forms one of the 44 subunits of the mitochondrial respiratory complex I (CI).¹ *NDUFA13* has a broad range of functions, the most important of which is maintaining the mitochondrial membrane potential by controlling CI assembly and activity.² *NDUFA13* is also known as gene associated with retinoid-interferon-induced mortality 19 and is reported to control interferon-beta and retinoic acid-induced cell death and expresses antioncogenic function negatively regulating signal transducer and transcription activator.³ The latter mediates cellular responses to cytokines and various growth

factors.³⁻⁵ *NDUFA13*-null mice result in embryonic lethality, whereas blastocysts with homozygous *NDUFA13* deletion show absent mitochondrial CI.⁶

CI deficiency is the most frequent early-onset mitochondrial oxidative phosphorylation (OXPHOS) disorder accounting for up to 30% of cases.⁷ Biallelic variants in *NDUFA13* have been associated with mitochondrial CI deficiency, nuclear type 28 in three affected individuals from two families.^{8,9} Currently, with only two families reported, the clinical and molecular spectrum of *NDUFA13*-related CI deficiency remains poorly characterized; hence, here, we report on further 10 affected individuals from 9 independent families with four rare missense and three predicted loss-of-function (LOF) biallelic *NDUFA13* variants and provide follow-up clinical-radiological details from the

previously reported families. Our study provides a cumulative phenotypic characterization of *NDUFA13*-related disease.

Materials and methods

Patient identification, genetic and clinical investigation

Using the GeneMatcher platform¹⁰ and extensive international data sharing, nine families reported here were identified. A uniform clinical proforma was distributed to obtain clinical details from new and previously reported families. Brain MRI was available in 12 individuals from 10 families and was reviewed by an experienced paediatric neuroradiologist (M.S.). Parents and legal guardians of all affected individuals gave their consent for the publication of clinical and genetic information according to the Declaration of Helsinki, and the study was approved by the respective local Ethics Committees.

Proband-only or trio exome sequencings were performed on DNA extracted from blood-derived leukocytes, followed by data analysis and variant filtration, and Sanger segregation analysis in 9 families in 6 different centres following the protocols described previously (Supplemental Table 1). Haplotype analysis was done using our ExHap tool. Briefly, VCF files of patients harbouring shared pathogenic variant were merged along with control samples. Using R, we plotted a colour banding plot to visualize genotype pattern of flanking regions of the variant site to infer homozygosity haplotypes.

The assessment of OXPHOS protein expression by western blotting and the evaluation of mitochondrial respiratory chain activities in fibroblasts

Skin biopsies were obtained from two families (Individuals 7 and 8), establishing explant cultures to grow primary fibroblast cell lines. Cells were prepared, alongside two paediatric control lines, for whole-cell lysates and subsequent SDS-PAGE/western blot analysis as described previously.¹¹ The assessment of mitochondrial respiratory chain enzyme activities was made in mitochondrial fractions as described previously.¹² See [Supplementary methods](#) for further details.

Protein modelling

The variants were considered in the context of cryo-EM human CI structure from PDB 5XTD.¹³ The conservation of the structure was evaluated by alignment to the ovine CI structure (PDB 6ZKC). The interactions of mutated residues were evaluated by considering polar interactions within the program PYMOL.

Literature review

We compiled a list of genes associated with CI deficiency using the Online Mendelian Inheritance in Man (OMIM) database. Multiple electronic databases including PubMed, Web of Science, and Google Scholar were screened with the search terms including ‘Complex I deficiency’, ‘NADH oxidoreductase’, ‘mitochondrial disease’ and the names of the target genes. All identified case reports and case series with original patient data published in English and providing phenotypic presentation were considered. Articles not related to CI deficiency and reviews, editorials and opinion pieces without original patient data were excluded. For each included study, we extracted relevant clinical details using a standardized data collection form. Extracted data were tabulated and analysed to identify common clinical patterns, genotype–phenotype correlations and variations in disease presentation among CI deficiency-associated genes. Based on the frequency of reported symptoms, we extracted core phenotypes for each CI deficiency-associated gene.

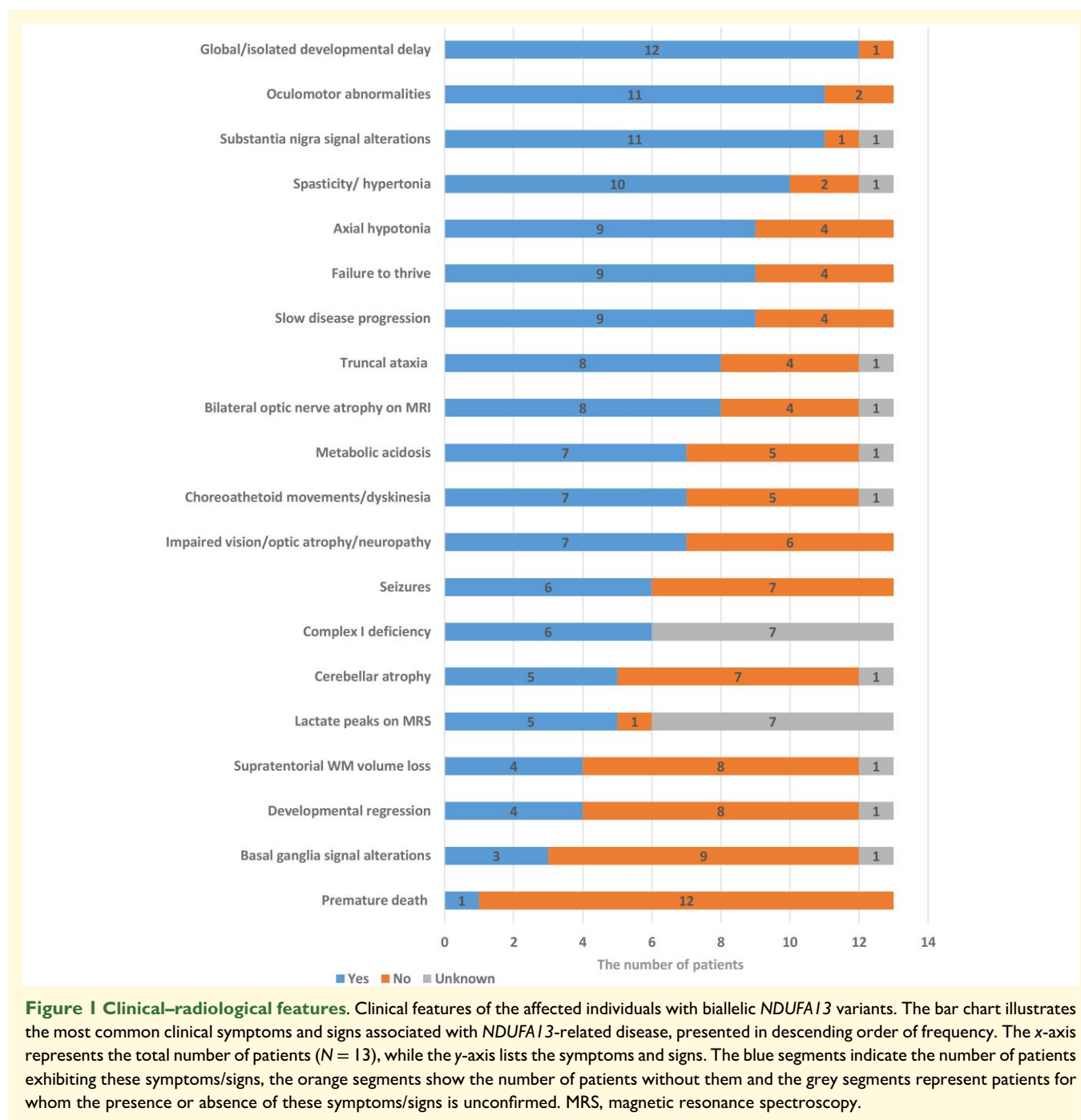
No statistical analysis was performed in this study.

Results

Clinical findings

The main phenotypic features of the present cohort and the previously reported individuals affected by *NDUFA13*-related disease are summarized in [Fig. 1](#), [Supplemental Tables 1](#) and [2](#). Detailed clinical history is provided in the supplemental case reports. Video recordings are available for families 1, 2, and 7 ([Videos 1–3](#)). The further clinical description will focus on 13 affected individuals from 11 unrelated families including 9 families found in the present study and two previously reported families with their follow-up details.^{8,9} There were 7 females and 6 males, 12 of whom are currently alive with a mean age of 7.8 ± 5.4 years (range 2.5–18). The disease was mostly infantile-onset (≤ 12 months) except for two affected individuals manifesting after the age of 18 months old (Families 2 and 8). The onset of the disease was more subtle and progressive, rather than being associated with decompensation during a somatic illness, vaccination or fever. In more than half of the individuals (8/13, 61%), the disease had slow rates of progression, whereas others displayed moderate (3/13, 23%) and rapid (2/13, 16%) rates of progression. The type of progression was determined subjectively by clinicians based on the degree of acquisition of milestones, regression, accumulation of symptoms and their severity and functional capacity. Failure to thrive was reported in most of the cohort (9/13, 69%). A history of metabolic acidosis was present in 7/12 (58%) individuals.

Developmental delay was severe-to-profound in 7/13 (54%), moderate in 5/13 (38%) and mild in 1/13 (8%) affected individuals. While eight affected individuals presented with global developmental delay, four affected individuals



had only isolated motor delay. Half of the affected individuals (7/13, 53%) had never attained independent walking, two affected individuals walked independently by 2 years old but then gradually lost independent ambulation, and three individuals were able to walk albeit with an ataxic gait. The speech was mostly limited to sounds only and babbling (7/13, 54%) except for the other six individuals who were able to talk.

The median age of the cohort at the most recent follow-up was 4.7 years (range, 2.3–17) where the affected individuals displayed moderate-to-severe intellectual disability (8/13,

61%), acquired microcephaly (4/13, 31%) and encephalopathy (6/13, 46%). Reduced visual acuity with bilateral optic atrophy or neuropathy (7/13, 54%) and oculomotor abnormalities (11/13, 84%) including nystagmus, slow saccades, ptosis and esotropia were among the frequent ocular signs. Cataracts were documented to be absent in 8/13 patients, and its presence is unknown in five. Neuromuscular phenotype included dysarthria (8/13, 61%), axial (9/13, 69%) and peripheral (6/12, 50%) hypotonia (in the infantile period) and spasticity/hypertonia (10/12, 83%). Movement disorders including choreoathetoid movements of the limbs and



Video 1 The video shows the patient from Family 1 who has axial hypotonia, increased deep tendon reflexes (DTRs) at the Achilles tendon and decreased DTRs at the knees with a likely positive Babinski sign on the left.



Video 2 The video shows an affected individual from Family 2 who has jerky neck flexion-extension movements in the neck and jerky movements in his shoulders. He is unable to stand unassisted.



Video 3 The video shows an affected individual from Family 7 who shows brisk DTRs from the lower limbs.

face (7/12, 58%), dyskinesia (7/12, 58%), bradykinesia (5/11, 45%) and truncal ataxia (8/12, 66%) were frequently displayed in the cohort. Hyperkinetic movement disorders tended to subside over time in 5/6 (83%) affected individuals. Generalized tonic-clonic or myoclonic seizures were reported in 6/13 (46%) individuals with seizure manifestation from the age of 3 months to 9 years. No pharmacoresistant seizures were reported.

Biochemical tests from serum and urine were available from 8 patients, which revealed increased serum lactate (7/8 patients with a mean serum lactate level of 4.1 ± 0.7 mmol/L; range, 3.2–5.0; normal levels <2 mmol/L) and increased serum or urine alanine (3/8). Lactate levels in the cerebrospinal fluid were available from 6/13 patients and were increased in two individuals (2.8 and 3 mmol/l, normal range -1.0 to 2.0 mmol/L). Only six individuals in the cohort underwent respiratory chain enzyme testing, either in muscle tissue or skin fibroblasts, which confirmed isolated CI deficiency in every case.

Nineteen brain MRI studies were available for review in 12 individuals from 10 families (mean age at first MRI, 2.4

years; range, 9 months to 7 years). Frequent neuroimaging features (Fig. 2) included bilateral symmetric T2 hyperintense lesions in the substantia nigra (11/12, 91.6%) and bilateral optic nerve atrophy (8/12, 66.6%). Faint signal alterations in the cerebellar dentate nuclei were noted in 7/12 cases (58.3%), while periaqueductal grey matter focal lesions were present in 6/12 affected individuals (50%). Mild cerebellar atrophy involving the lateral or superior portions of the cerebellar hemispheres was depicted in 5/12 individuals (41.6%). Tectal plate lesions were noted in 4/12 individuals (33.3%), while central midbrain lesions were present in 3/12 (25%) cases. Supratentorial white matter volume loss and faint periventricular signal alterations were seen in 4/12 individuals (33.3%). Additional findings included multiple basal ganglia lesions (3/12, 25%), signal alterations in the inferior olivary nuclei and/or medulla (3/12, 25%), central tegmental tracts (2/12, 16.6%) and cervical spinal cord (1/12, 8.3%). Diffusion-weighted imaging was performed in 10 individuals and 12/19 MRI studies: focal areas of restricted diffusion were depicted in 5/12 studies at the level of the basal ganglia, left frontal white matter, substantia nigra and periaqueductal grey matter. All focal lesions were small (≤ 5 mm). MR spectroscopy was performed in three individuals and 6/19 MRI studies: high lactate peaks were noted at the level of the basal ganglia in 5/6 studies. Head CT was performed in two individuals and showed no intracranial calcifications. Longitudinal brain MRIs were available in six cases (two studies in five cases; three studies in one subject), at a median age of 1.8 years (IQR, 1–2.7 years) at first imaging and of 4.5 years (IQR, 2.7–8.2 years) at last follow-up. These studies revealed a reduction of the signal alterations in the brainstem ($n = 5$), progressive cerebellar atrophy ($n = 4$) and basal ganglia signal alterations with atrophy ($n = 1$). Subjects with cerebellar atrophy were all older than 5 years of age.

Genetic findings

Molecular genetic findings included seven *NDUFA13* variants, including four missense and three predicted LOF

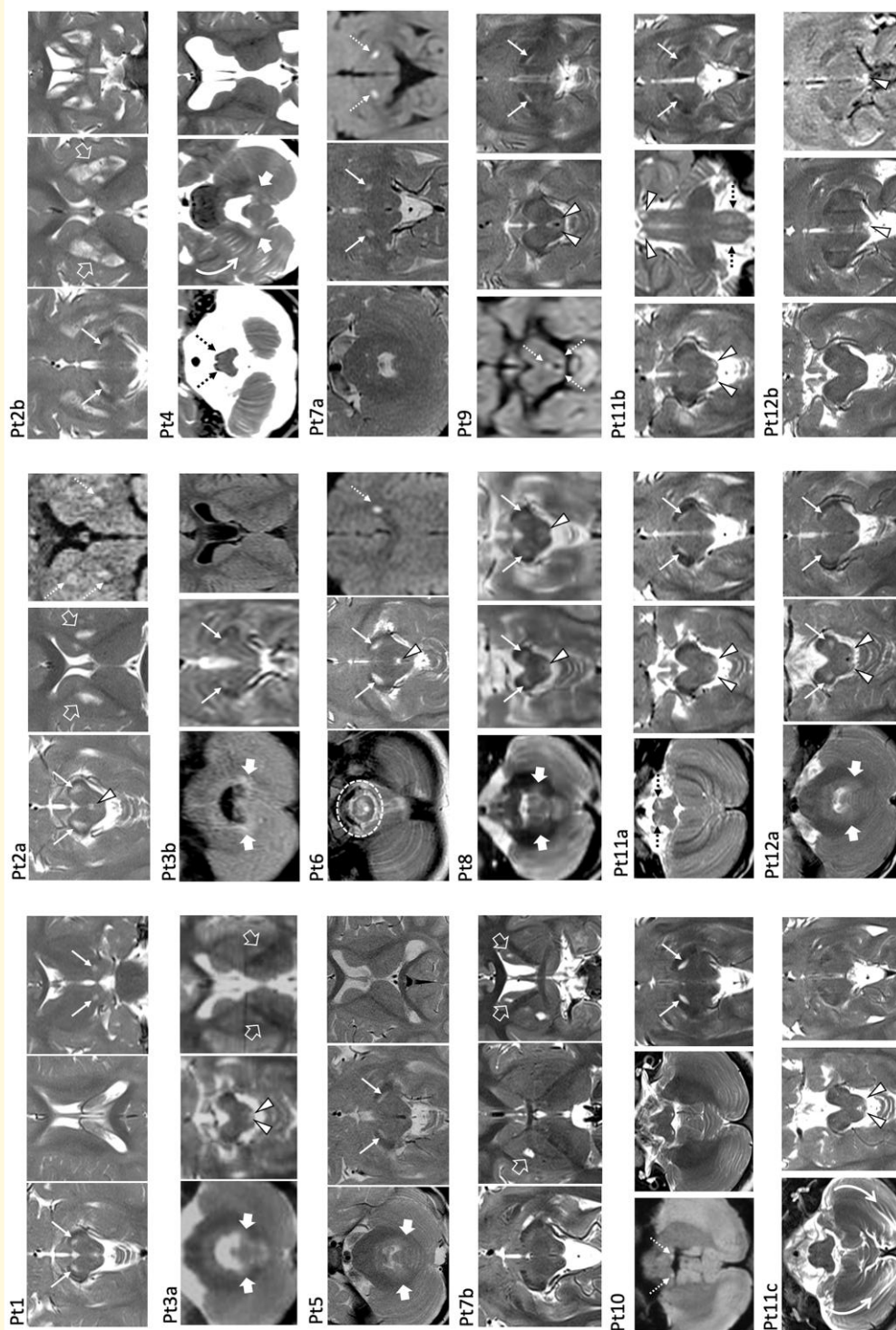


Figure 2 Neuroimaging features of NDUFA13-related disease. Most of the individuals present symmetric T2-hyperintense lesions of the substantia nigra (thin white arrows). These lesions are less evident on follow-up scans, as seen in Patient 2b, Patient 7b, and Patient 11b and c and Patient 12b). Periaqueductal and central midbrain signal alterations are visible in individuals Patient 3, Patient 6, Patient 9, Patient 11 and Patient 12 (white arrowheads). In three patients (Patient 2, Patient 3 and Patient 7), there are additional basal ganglia signal alterations (empty white arrows), which increase over time with associated atrophy in individual Patient 2, as depicted in Patient 2b. Faint T2 hyperintensities of the dentate nuclei are noticed in individuals Patient 3, Patient 4, Patient 5, Patient 8 and Patient 12 (thick white arrows). Subtle inferior olivary nuclei T2 hyperintensity is visible in individuals Patient 4 and Patient 11 (dashed black arrows). In one individual (Patient 6), there are T2 signal alterations at the level of the cervical spinal cord (dashed oval). Small foci of restricted diffusion (dashed white arrows) are noted in the right basal ganglia and bilateral substantia nigra (Patient 2a), left periventricular frontal white matter (Patient 6), bilateral substantia nigra (Patient 9), periaqueductal grey matter (Patient 9) and posterior medullary white matter tracts (Patient 10). Note: mild cerebellar atrophy mainly involving the cerebellar hemispheres in Patient 4 and Patient 11c). Pt, patient.

variants. Families 1, 3, 4, 7 and 9 carried a previously reported (in Family 10) pathogenic homozygous variant in exon 2 of *NDUFA13* (NM_015965.7) c.170G>A, p.(Arg57His). We analysed the haplotypes of this variant in three unrelated families, and the results revealed no shared haplotype, indicating that this variant likely recurred independently. (Supplementary Fig. 1). Family 8 harboured a homozygous predicted-deleterious missense variant c.164G>C, p.(Arg55Pro). Family 9 harboured a heterozygous missense c.187G>A, p.(Glu63Lys) variant in *trans* with the recurrent *NDUFA13* c.170G>A variant. Interestingly, the *NDUFA13* c.187G>A, p.(Glu63Lys) variant identified in Family 9 in a heterozygous state was also found in a patient with limb malformation and skeletal dysplasia and congenital glaucoma, but in a homozygous state (Individual 14, Family 12). This patient underwent diagnostic exome sequencing, which revealed the *NDUFA13* c.187G>A, p.(Glu63Lys) as a rare homozygous variant. We considered this phenotype an outlier; therefore, we have not included this case in the description of the main cohort. However, the case report for this patient is available in the supplementary material. Family 5 harboured an ultra-rare predicted deleterious missense *NDUFA13* c.107T>C, p.(Leu36Pro) variant, which was in *trans* with a splicing c.94+1G>A variant in *NDUFA13*. The missense c.107T>C, p.(Leu36Pro) variant was previously reported in the published Family 11. Family 2 harboured a novel homozygous frameshift variant c.7del, p.(Ala3ArgfsTer4) and Family 6 carried a homozygous protein-truncating variant that occurred at the beginning of the *NDUFA13* amino acid sequence c.22C>T, p.(Gln8*). The variants segregated with the disease in all newly reported nine families (Fig. 3A) and are either absent or observed as heterozygous in extremely low frequencies in publicly available and private variant frequency databases (Supplementary Table 3). All three LOF *NDUFA13* variants reported in the present study are located within exon 1 or at the exon 1-intron 1 boundary (Fig. 3B), and on the protein level, these LOF variants reside at the N-terminal matrix end or the C-terminal intermembrane space domain of the protein (Fig. 3C). The recurrent missense *NDUFA13* variant c.170G>A, p.(Arg57His) occurred at a highly conserved amino acid residue while the other three missense variants (Leu36, Arg55, Glu63) at moderately conserved residues, all with various *in silico* tools predicting a deleterious/damaging effect (Fig. 3D). All variants are within large regions of homozygosity. The homozygous splicing variant c.94+1G>A is predicted to affect splicing by alteration of the wild-type donor site between exons 1 and 2 (retrieved from SpliceAI server; Supplementary Fig. 2). The characteristics of the variants are summarized in Supplementary Table 3. No additional biallelic variants of likely pathogenic significance were identified in the cohort.

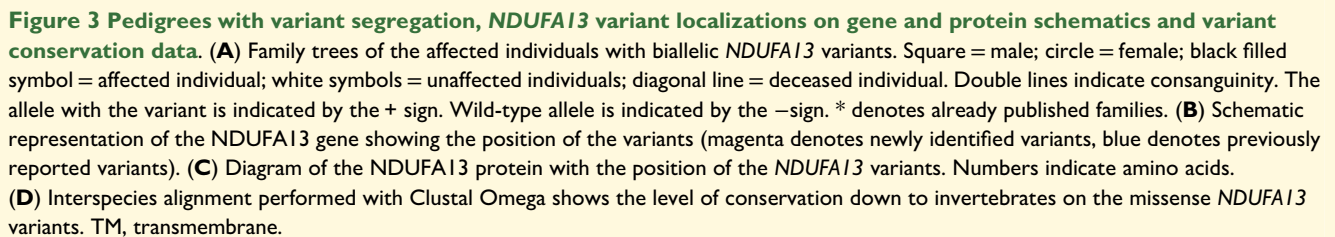
Genotype–phenotype correlation

Although families carrying the recurring *NDUFA13* c.170G>A, p.(Arg57His) variant shared features such as

infantile disease manifestation, slow disease progression rates, moderate-to-severe global developmental delay and failure to acquire independent gait, there was a noticeable variation in the development of epileptic seizures, movement disorders and regression. Individuals with the LOF *NDUFA13* variants exhibited isolated motor delay with preserved cognitive function, whereas all homozygous carriers of the recurrent *NDUFA13* c.170G>A, p.(Arg57His) variant were cognitively impaired as part of their global developmental delay. Additionally, affected individuals with p.(Arg57His) tended to have slower disease progression rates when compared with the carriers of the LOF *NDUFA13* variants. Carriers of the other missense variant in *NDUFA13* presented with a milder phenotype. No clear correlation between genotype and neuroimaging features was observed. The homozygous carrier of the c.187G>A, p.(Glu63Lys) variant in *NDUFA13* presented with limb malformation and skeletal dysplasia and congenital glaucoma phenotype only, whereas the association of the same variant with the recurrent *NDUFA13* variant c.170G>A in a *trans*-state compound heterozygosity resulted in a neurological phenotype.

The evaluation of the structural background of the variants

We analysed the structural background of the altered residues and explored potential reasons for their harmful effects (Fig. 4A and B). Most of these variant residues are conserved across mammals, except for Leu36, which is replaced by Phe in most other species. The *NDUFA13* subunit and its environment are also highly conserved (e.g. PDB 6ZKC¹⁴). Subunit *NDUFA13* is tightly integrated within the complex at its ‘back’ at the junction of the peripheral and membrane arms (Fig. 4A). Here, it crosses the membrane from the matrix to IMS with one TM helix and interacts with many subunits, including core ND1 and NDUF58, as well as accessory *NDUFA3*. All the altered residues interact with neighbouring subunits (Fig. 4B), likely contributing to the stability of this critical region, which connects the enzyme’s two arms. Leu36 forms hydrophobic contacts with NDUF58 at the top of *NDUFA13*’s TM helix. Its substitution with Pro weakens these contacts and is likely to disrupt the helical structure of *NDUFA13* in this area. Arg55 and Arg57 are located at the C-terminal end of the *NDUFA13* TM helix. Arg55 forms hydrogen bonds with the backbone oxygen of Ile311 and Ser312 from *NDUFA3*. Replacing Arg55 with Pro will disrupt both these bonds and the local helical structure. Arg57 forms hydrogen bonds with the backbone oxygen of Ser157 in the ND1 subunit and interacts with Asn54 in *NDUFA13*, locally stabilizing its TM helix. The Arg57 alteration to His is expected to destabilize this region. Subunit ND1 forms the main core of the junction between the two arms and also lines the quinone-binding cavity, which may explain the particular severity of the Arg57His variant. Lastly, Glu63 forms a hydrogen bond or weak salt bridge with Arg101 from the *NDUFA3* subunit, likely stabilizing the exposed helices of *NDUFA3* at



Cultured fibroblasts were obtained from the proband of Family 6 (Individual 7) and Family 7 (Individual 8). Both individual's fibroblast samples demonstrated a specific decrease in the activity of mitochondrial CI activity: Individual 7: 0.120 nmols NADH oxidized.min⁻¹.unit

citrate synthase⁻¹, controls 0.197 ± 0.034 (mean \pm SD, $n = 8$); Individual 8: 0.072 nmols NADH oxidized.min⁻¹.unit citrate synthase⁻¹, controls 0.197 ± 0.034 (mean \pm SD, $n = 8$) Furthermore, western blot analyses of key OXPHOS components showed a marked decrease in the steady-state levels of NDUFB8, another important CI subunit, whilst subunits of complex II (SDHA), complex III (UQCRC2) and complex V (ATP5A) were relatively unchanged. We did also note an apparent increase, possibly as a compensatory mechanism, in the steady-state level of the complex IV subunit COXII in both individuals (Fig. 4C).

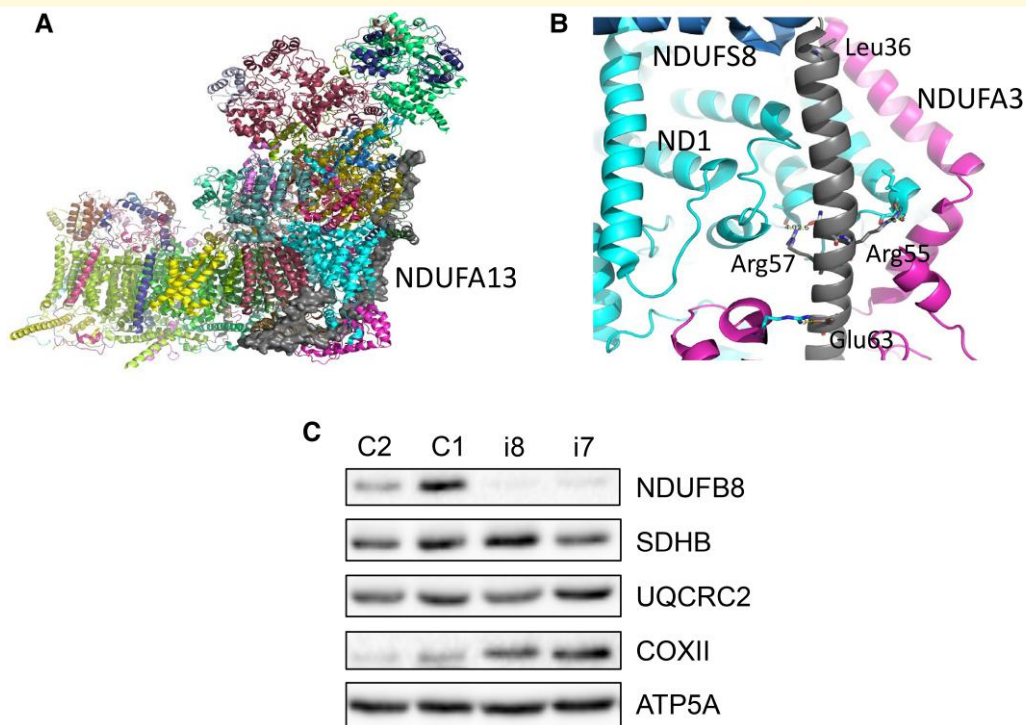


Figure 4 Structural background of NDUF13 variants and biochemical assessment of fibroblasts from individuals with biallelic NDUF13 variants. (A) Overview of human complex I (PDB 5XTD).¹³ View from the 'back', with membrane arm horizontal. Subunits are shown as cartoons and coloured differently. NDUF13 subunit is highlighted as grey surface. (B) Interactions of NDUF13 (grey) residues with neighbouring subunits ND1 (cyan), NDUF3 (magenta) and NDUF8 (blue). (C) Western blot analysis of OXPHOS components in individual (i7 and i8) and control (C1–2) fibroblasts (Supplementary Fig. 3 for source data). C, control; I, individual; NDUF8, NADH-ubiquinone oxidoreductase iron-sulfur protein 8; NDUF3, NADH-ubiquinone oxidoreductase subunit A3; NDUF8, ND1, NADH dehydrogenase I; NDUF8, NADH-ubiquinone oxidoreductase subunit B8; SDHB, succinate dehydrogenase complex, iron-sulfur subunit B; UQCRC2, ubiquinol-cytochrome c reductase core protein II; COXII, cytochrome c oxidase subunit 2; ATP5F1A, ATP synthase f1, subunit alpha.

Literature review

We compiled the results of an extensive literature review, uniformly collecting the clinical details of all reported patients with isolated CI deficiency caused by 43 disease genes encoding CI subunits and assembly factors (Supplementary Table 4). Our analysis has shown that the clinical presentation of CI deficiency is incredibly heterogeneous, but the most common phenotype includes neurodevelopmental delay and hypotonia, frequently associated with lactic acidosis. Based on the frequency of reported symptoms and signs, we were able to identify a discernible core phenotype for genes with many reported families and thorough phenotyping. For example, our analysis revealed that, in addition to neurodevelopmental delay and hypotonia, frequent signs of NDUFV1-related disease (OMIM no. 618225) include spasticity, seizures, nystagmus and respiratory insufficiency. Dystonia is a frequent feature of NDUF8 (OMIM no. 618224), NDUF9 (OMIM no. 618247), NDUF10 (OMIM no. 618243) and NDUF5-related diseases (OMIM no. 618238). The combination of dystonia and cerebellar ataxia is seen in NDUF6 (OMIM no. 618239) and NDUF12-related diseases (OMIM no. 618244), while

cerebellar ataxia is common in NDUF1 (OMIM no. 301020). Spastic ataxia is a common feature of NDUF13 (OMIM no. 618249) and NUBPL (OMIM no. 618242). Cardiomyopathy is frequently seen in NDUF11 (OMIM no. 301021), NDUF8 (OMIM no. 618222), NDUFV2 (OMIM no. 618229) and ACAD9 (OMIM no. 611126) defects. CI deficiency, associated with the following genes results in high mortality rates: NDUF1 (OMIM no. 618226), NDUF2 (OMIM no. 618228), NDUF4 (OMIM no. 252010), NDUF1 (OMIM no. 618234) and MT-ND3 (OMIM no. 516002).

Discussion

Isolated deficiency of CI is the most commonly identified biochemical defect in childhood-onset mitochondrial disease, accounting for approximately a third of all cases of OXPHOS disorders.⁷ CI deficiency is clinically heterogeneous, but most affected individuals develop symptoms during the first year of life and have a rapidly progressive disease course, resulting in a fatal outcome in childhood.^{7,15,16} The most prevalent clinical presentations of CI deficiency

include Leigh syndrome, leukoencephalopathy and various early-onset neurodegenerative disorders.⁷ There are >40 disease genes encoding structural subunits and assembly factors associated with mitochondrial CI deficiency.¹⁷ So far, no definitive correlation has been identified between the clinical phenotype and defects in CI subunits and assembly factors.¹⁸ However, it is important to consider that most genes leading to CI deficiency have been reported in only a small number of patients. This, combined with the variable degree of phenotyping among these patients, prevents us from seeing a full clinical spectrum for each gene associated with CI deficiency and from establishing a genotype–phenotype correlation. This was confirmed by our literature review, as we were able to suggest a core clinical phenotype specifically for those isolated CI deficiency-causing genes that had multiple reported families and detailed phenotyping. The purpose of our literature review was to identify a potential genotype–phenotype correlation and determine the core phenotype for each isolated CI deficiency-associated gene that might aid clinicians and medical geneticists in diagnosis.

Given the typically heterogeneous clinical presentation of CI deficiency, the phenotype of the previously reported individuals with biallelic variants in *NDUFA13* ranged from an infantile-onset slowly progressive encephalopathy with severe optic neuropathy, retinal dysfunction and prolonged survival without extra-neurological involvement in one family to Leigh syndrome in another. Isolated CI enzyme defect was found in skin fibroblast and muscle samples from three individuals.^{8,9} Our cumulative phenotypic analysis of nine new and two previously reported families suggested that the phenotype of defective *NDUFA13* encompasses mostly infantile-onset and non-rapidly progressing neurological impairment on the background of severe-to-profound and moderate global and isolated developmental delay. Spasticity, cerebellar ataxia, frequent movement disorders, optic nerve atrophy and subtle neuroimaging features related to Leigh syndrome with increased lactate were noted in most affected individuals. In particular, the most affected region was the substantia nigra as previously reported in other disorders of the oxidative phosphorylation system,¹⁹ followed by the periaqueductal grey matter, central midbrain, pons, medulla and basal ganglia with possible associated small areas of restricted diffusion. Notably, basal ganglia involvement was less frequent in subjects with *NDUFA13* variants compared to other CI deficiency disorders, i.e. 25% versus 90% of cases reported by Lebre *et al.*²⁰ Moreover, while cerebellar cortical involvement is more common in Leigh syndrome due to variants in mtDNA genes,^{19,20} we found mild cerebellar atrophy in about 40% of *NDUFA13* cases after the age of 5 years. Finally, differently from other CI nuclear gene variants,^{19–21} cavitating leukoencephalopathy was not present in our series and white matter signal alterations were subtle and non-specific in all cases.

The sole limb malformation and skeletal dysplasia and congenital glaucoma phenotype in a patient with the homozygous *NDUFA13* c.187G > A, p.(Glu63Lys) variant could

suggest that this variant is most probably hypomorphic. Although this missense variant has consistently been predicted to be deleterious and damaging in several *in silico* tools and has high GERP (4.5) and CADD (25.5) scores, in contrast to other *NDUFA13* variants reported in our study, its allele frequency in gnomAD Version 4 is 0.00003904, making an overall of 63 alleles out of 1 613 838. The variant is enriched within South Asian and European (non-Finish) populations. Hypomorphic variants are typically associated with milder clinical presentations due to only partial loss of normal gene function^{22,23} and require the presence of another pathogenic variant on the opposite allele to express a phenotype. Although some studies suggest that mitochondrial diseases could primarily manifest with skeletal phenotypes²⁴ and congenital glaucoma,²⁵ the role of the *NDUFA13* c.187G > A, p.(Glu63Lys) variant in the limb malformation and skeletal dysplasia and congenital glaucoma phenotype observed in Family 12 remains unclear.

Akin to most of the CI-deficient patients, the present cohort did not have dysmorphic features and were non-syndromic, with mostly normal pregnancy and birth parameters.²⁶

In contrast to other CI deficiency syndromes, a slow disease progression with longer survival was suggested in previous *NDUFA13* reports suggesting a possible antiapoptotic effect of defective *NDUFA13*, the function mentioned previously.^{8,9} Interestingly, slow disease progression in our nine new families presenting with a neurological phenotype was in concordance with the previous reports highlighting the assumption that biallelic variants in *NDUFA13* might have less severe functional consequences than variants in other genes associated with CI deficiency.^{8,9} Alternatively, the broad range of *NDUFA13* functions might have influenced the rates of disease progression.^{8,9}

Our protein modelling data suggest that the missense *NDUFA13* variants reported in this study are likely to weaken the tight interaction network of several subunits at the critical junction between the two arms of the complex. This weakening could lead to defective assembly and a reduction in the amount of functional complex. The mechanism that couples redox reactions with proton pumping in CI relies on large, coordinated conformational changes around the quinone-binding site, located at the interface between the peripheral and membrane arms.^{14,27} Any destabilization of this interface due to alterations in *NDUFA13* will result in reduced activity due to suboptimal coupling. The overall consequence of defective assembly and impaired coupling would be a diminished contribution of CI to mitochondrial energy production.

Similar to the previous reports of affected individuals with biallelic variants in *NDUFA13*, fibroblasts in the present study showed a marked decrease in *NDUFA13* protein as well as other CI subunits and a decrease in the assembly of the CI holoenzyme.^{8,9} Individual 8, harbouring the same *NDUFA13* c.170G > A, p.(Arg57His) variant as previously reported, had some residual *NDUFA13* protein levels, which is in accordance with the reported individuals.⁸ Interestingly, both affected individuals also displayed an increase in

steady-state levels of complex IV protein subunits and an increase in complex IV activity. A previous study on Individual 11 also saw an increase of complex IV by BN-PAGE.⁹

Overall, our study expands the phenotypic and genetic spectrum of *NDUFA13*-related CI deficiency based on data from 13 affected individuals. The description of additional cases will further advance our understanding of *NDUFA13* defects in humans.

Supplementary material

Supplementary material is available at *Brain Communications* online.

Acknowledgements

We thank all individuals and relatives for consent to be part of the study. Families 1–4, 7, were collected as part of the SYNAPS Study Group collaboration funded by The Wellcome Trust and strategic award (Synaptopathies) funding (WT093205 MA and WT104033AIA), and research was conducted as part of the Queen Square Genomics group at the University College London, supported by the National Institute for Health Research University College London Hospitals Biomedical Research Centre. We are also grateful to Queen Square Genomics at the Institute of Neurology University College London, supported by the National Institute for Health Research University College London Hospitals Biomedical Research Centre, for the bioinformatics support. For the purpose of Open Access, the author has applied a CC BY public copyright license to any Author Accepted Manuscript version arising from this submission.

Funding

This study was funded by the Medical Research Council (MR/S01165X/1, MR/S005021/1, G0601943). The Medical Research Council (MR/S01165X/1, MR/S005021/1, MRC ICGNMD), Wellcome Trust 221951/Z/20/Z, Global Parkinson's Genetics Program, Aligning Science Across Parkinson's, The Michael J. Fox Foundation, The National Institute for Health Research University College London Hospitals Biomedical Research Centre, Rosetree Trust, Multiple System Atrophy Trust, Brain Research UK, Sparks Great Ormond Street Hospital Charity, Muscular Dystrophy, Muscular Dystrophy Association United States of America, and King Baudouin Foundation. H.T. was supported by the European Union's Seventh Framework Programme for research, technological development and demonstration under grant agreement no. 608473. M.S.A.-H. is funded by the Science and Technology Development Fund Academy of Science Research and

Technology Egypt (Grant number: 33492, Ethical approval number: 20066). R.W.T. is funded by the Wellcome Centre for Mitochondrial Research (203105/Z/16/Z), the Mitochondrial Disease Patient Cohort (UK) (G0800674), the Medical Research Council International Centre for Genomic Medicine in Neuromuscular Disease (MR/S005021/1), the Medical Research Council (MR/W019027/1), the Lily Foundation, Mito Foundation, the Pathological Society, LifeArc, the UK National Institute for Health Research Biomedical Research Centre for Ageing and Age-related disease award to the Newcastle upon Tyne Foundation Hospitals NHS Trust and the UK NHS Highly Specialised Service for Rare Mitochondrial Disorders of Adults and Children. H.H. and R.K. are supported by Global Parkinson's Genetic Program and The Michael J. Fox Foundation Grant ID: MJFF-022153.

Competing interests

D.A.C. and M.N. are employees of GeneDx, LLC.

Data availability

The authors have not generated any codes for this work. As such, there are no datasets or code repositories associated with this study.

References

1. Wirth C, Brandt U, Hunte C, Zickermann V. Structure and function of mitochondrial complex I. *Biochim Biophys Acta*. 2016;1857(7):902-914.
2. Lu H, Cao X. GRIM-19 is essential for maintenance of mitochondrial membrane potential. *Mol Biol Cell*. 2008;19(5):1893-1902.
3. Angell JE, Lindner DJ, Shapiro PS, Hofmann ER, Kalvakolanu DV. Identification of GRIM-19, a novel cell death-regulatory gene induced by the interferon-beta and retinoic acid combination, using a genetic approach. *J Biol Chem*. 2000;275(43):33416-33426.
4. Seo T, Lee D, Shim YS, et al. Viral interferon regulatory factor 1 of Kaposi's sarcoma-associated herpesvirus interacts with a cell death regulator, GRIM19, and inhibits interferon/retinoic acid-induced cell death. *J Virol*. 2002;76(17):8797-8807.
5. Zhang J, Yang J, Roy SK, et al. The cell death regulator GRIM-19 is an inhibitor of signal transducer and activator of transcription 3. *Proc Natl Acad Sci U S A*. 2003;100(16):9342-9347.
6. Huang G, Lu H, Hao A, et al. GRIM-19, a cell death regulatory protein, is essential for assembly and function of mitochondrial complex I. *Mol Cell Biol*. 2004;24(19):8447-8456.
7. Fassone E, Rahman S. Complex I deficiency: Clinical features, biochemistry and molecular genetics. *J Med Genet*. 2012;49(9):578-590.
8. Angebault C, Charif M, Guegen N, et al. Mutation in *NDUFA13*/GRIM19 leads to early onset hypotonia, dyskinesia and sensorial deficiencies, and mitochondrial complex I instability. *Hum Mol Genet*. 2015;24(14):3948-3955.

9. Gonzalez-Quintana A, Garcia-Consuegra I, Belanger-Quintana A, *et al.* Novel NDUFA13 mutations associated with OXPHOS deficiency and Leigh syndrome: A second family report. *Genes (Basel)*. 2020;11(8):855.
10. Sobreira N, Schiettecatte F, Valle D, Hamosh A. GeneMatcher: A matching tool for connecting investigators with an interest in the same gene. *Hum Mutat*. 2015;36(10):928-930.
11. Thompson K, Majd H, Dallabona C, *et al.* Recurrent de novo dominant mutations in SLC25A4 cause severe early-onset mitochondrial disease and loss of mitochondrial DNA copy number. *Am J Hum Genet*. 2016;99(4):860-876.
12. Kirby DM, Thorburn DR, Turnbull DM, Taylor RW. Biochemical assays of respiratory chain complex activity. *Methods Cell Biol*. 2007;80:93-119.
13. Guo R, Zong S, Wu M, Gu J, Yang M. Architecture of human mitochondrial respiratory megacomplex I2III2IV2. *Cell*. 2017;170(6):1247-1257.e12.
14. Kampjut D, Sazanov LA. The coupling mechanism of mammalian respiratory complex I. *Science*. 2020;370(6516):eabc4209.
15. Bjorkman K, Sofou K, Darin N, *et al.* Broad phenotypic variability in patients with complex I deficiency due to mutations in NDUFS1 and NDUFV1. *Mitochondrion*. 2015;21:33-40.
16. DiMauro S, Emmanuele V. The clinical spectrum of nuclear DNA-related mitochondrial disorders. In: *Mitochondrial disorders caused by nuclear genes*. Springer; 2013:3-25.
17. Fernandez-Vizarra E, Zeviani M. Mitochondrial disorders of the OXPHOS system. *FEBS Lett*. 2021;595(8):1062-1106.
18. Rodenburg RJ. Mitochondrial complex I-linked disease. *Biochim Biophys Acta*. 2016;1857(7):938-945.
19. Alves CAPF, Teixeira SR, Martin-Saavedra JS, *et al.* Pediatric Leigh syndrome: Neuroimaging features and genetic correlations. *Ann Neurol*. 2020;88(2):218-232.
20. Lebre AS, Rio M, Faivre d'Arcier L, *et al.* A common pattern of brain MRI imaging in mitochondrial diseases with complex I deficiency. *J Med Genet*. 2011;48(1):16-23.
21. Roosendaal SD, van de Brug T, Alves CAPF, *et al.* Imaging patterns characterizing mitochondrial leukodystrophies. *AJNR Am J Neuroradiol*. 2021;42(7):1334-1340.
22. Indelicato E, Boesch S, Zech M. Reply to: Early onset nonprogressive generalized dystonia is caused by biallelic SHQ1 variants. *Mov Disord*. 2023;38(6):1119-1120.
23. Simon MT, Eftekharian SS, Ferdinandusse S, *et al.* ECHS1 disease in two unrelated families of samoan descent: Common variant—Rare disorder. *Am J Med Genet A*. 2021;185(1):157-167.
24. Zhao T, Goedhart C, Pfeffer G, *et al.* Skeletal phenotypes due to abnormalities in mitochondrial protein homeostasis and import. *Int J Mol Sci*. 2020;21(21):8327.
25. Finsterer J, Zarrouk-Mahjoub S, Daruich A. The eye on mitochondrial disorders. *J Child Neurol*. 2016;31(5):652-662.
26. Distelmaier F, Koopman WJ, van den Heuvel LP, *et al.* Mitochondrial complex I deficiency: From organelle dysfunction to clinical disease. *Brain*. 2009;132(Pt 4):833-842.
27. Kravchuk V, Petrova O, Kampjut D, *et al.* A universal coupling mechanism of respiratory complex I. *Nature*. 2022;609(7928):808-814.